Journal of Quantitative Spectroscopy & Radiative Transfer 206 (2018) 46–54

Contents lists available at ScienceDirect

Journal of Quantitative Spectroscopy & Radiative Transfer

journal homepage: www.elsevier.com/locate/jqsrt

The 1943 K emission spectrum of $H_2{}^{16}O$ between 6600 and 7050 cm^{-1}

Eszter Czinki[a], Tibor Furtenbacher[a], Attila G. Császár[a,*], André K. Eckhardt[b], Georg Ch. Mellau[c,*]

[a] MTA-ELTE Complex Chemical Systems Research Group and Laboratory of Molecular Structure and Dynamics, Institute of Chemistry, Eötvös Loránd University, Budapest 112, P.O. Box 32, H-1518, Hungary
[b] Institut für Organische Chemie, Justus-Liebig-Universität Gießen, Heinrich-Buff-Ring 17, Gießen D-35392, Germany
[c] Physikalisch-Chemisches Institut, Justus-Liebig-Universität Gießen, Heinrich-Buff-Ring 17, Gießen D-35392, Germany

ARTICLE INFO

Article history:
Received 9 August 2017
Revised 28 October 2017
Accepted 30 October 2017
Available online 1 November 2017

Keywords:
Water vapor
High-resolution emission spectroscopy
Transition wavenumbers
Energy levels
MARVEL
Spectroscopic database
Infrared spectra
SyMath

ABSTRACT

An emission spectrum of $H_2{}^{16}O$ has been recorded, with Doppler-limited resolution, at 1943 K using Hot Gas Molecular Emission (HOTGAME) spectroscopy. The wavenumber range covered is 6600 to 7050 cm^{-1}. This work reports the analysis and subsequent assignment of close to 3700 $H_2{}^{16}O$ transitions out of a total of more than 6700 measured peaks. The analysis is based on the Measured Active Rotational-Vibrational Energy Levels (MARVEL) energy levels of $H_2{}^{16}O$ determined in 2013 and emission line intensities obtained from accurate variational nuclear-motion computations. The analysis of the spectrum yields about 1300 transitions not measured previously and 23 experimentally previously unidentified rovibrational energy levels. The accuracy of the line positions and intensities used in the analysis was improved with the spectrum deconvolution software SyMath via creating a peak list corresponding to the dense emission spectrum. The extensive list of labeled transitions and the new experimental energy levels obtained are deposited in the Supplementary Material of this article as well as in the ReSpecTh (http://www.respecth.hu) information system.

1. Introduction

Water is the most abundant polyatomic molecule in the universe. The spectroscopic detection and quantification of the amount of water vapor in different environments is a fundamental task in several areas of chemistry, spectroscopy, astronomy, and remote sensing. Due to the numerous analytical applications there is strong interest in the detailed laboratory investigation of the high-resolution spectra of water vapor from the microwave to the ultraviolet [1–7]. For $H_2{}^{16}O$, more than 100 experimental high-resolution spectroscopic studies have been published, Tennyson et al. [4] provides a hopefully complete list up to 2013. These measurements provide an excellent coverage of the rovibrational levels of $H_2{}^{16}O$ up to 15 000 cm^{-1}. This coverage extends significantly above the barrier to linearity of $H_2{}^{16}O$, which is about 11 100 cm^{-1} [8–11]. Transitions covering the highly excited levels beyond 15 000 cm^{-1} have been measured only sporadically, though gradually more and more energy levels have become available up to the first dissociation limit [12] and even beyond [13,14].

For analytical applications of high-resolution molecular spectroscopy a list of transition wavenumbers and intensities are needed, their collection is often referred to as a line list. For some triatomic molecules, most notably HCN, it is possible to cover experimentally the complete list up to very high energy with a relative accuracy better than 10^{-7} [15,16]. The existence of a list in which not a single eigenenergy of the molecular system is missing, combined with highly accurate *ab initio* intensity computations, allows accurate analytical analysis of HCN sources even at high temperatures. The measurement and the analysis of the HCN eigenenergies originates from a single laboratory; this ensures the internal consistency and accuracy of the eigenenergy list.

For water, experimental data sets have been reported by many laboratories, they are based on different experiments with transitions measured with very different accuracy and precision. The more than 100 data sets highly overlap and the eigenenergies reported in the individual sources have been based on a limited number of experiments. As part of an IUPAC-sponsored research effort [4,5,17–19] the complete set of so far published experimental spectroscopic information obtained from the assignment of high-resolution absorption and emission spectra for nine water isotopologues, $H_2{}^{16}O$, $H_2{}^{17}O$, $H_2{}^{18}O$, $HD^{16}O$, $HD^{17}O$, $HD^{18}O$, $D_2{}^{16}O$, $D_2{}^{17}O$,

* Corresponding authors.
E-mail addresses: csaszar@chem.elte.hu (A.G. Császár), georg@mellau.de (G.Ch. Mellau).

https://doi.org/10.1016/j.jqsrt.2017.10.028
0022-4073/

and $D_2{}^{18}O$, has been collected and analyzed. The experimental spectroscopic knowledge has been organized based on the concept of spectroscopic networks (SN) [20–22]. The conversion of the measured rovibrational transitions to energy levels is based on the MARVEL (Measured Active Rotational-Vibrational Energy Levels) protocol [22–25] built upon the idea of SNs, while utilizing heavily first-principles computed data [26,27]. The current MARVEL list of $H_2{}^{16}O$ eigenenergies [4] is complete up to 7500 cm^{-1}.

High-temperature water spectra contain a huge number of transitions not observed and/or assigned to date. The analysis of hot spectra allows the characterization of new energy levels and can extend significantly the database of rovibrational levels. Accurate transition wavenumbers for which the lower and upper levels have already been determined can improve substantially the accuracy of the eigenenergies determined via the MARVEL protocol. The most significant contribution to this improvement comes from transitions connecting lower and upper levels defining new spectroscopic basic cycles [28] and from transitions connecting energy level sets of different previous measurements or those determined from measurements with low accuracy. In this work we report the analysis of a near-infrared water emission spectrum in which we assigned about 4000 transitions, connecting for the first time many previously determined energy levels. Including these transitions in the MARVEL protocol we have improved the accuracy of the energies of many highly excited rovibrational states, where the previous accuracy was only about 0.02 cm^{-1} (see Section 4.5 below).

A number of spectroscopic studies exists [8,29–50] investigating warm (between 400 and 700 K) and hot (up to 3000 K) $H_2{}^{16}O$ spectra. The hottest emission spectra of $H_2{}^{16}O$ have been recorded in the laboratory in an oxy-acetylene flame at about 3000 K [46], while the absorption spectra recorded in sunspots correspond to a temperature of about 3200 K [51]. Sunspots provide a very rich source of spectroscopic data on water [40], and many lines, which are almost certainly due to hot water, still need to be assigned. Hot spectra are rich in relatively high-J (where J is the quantum number corresponding to the overall rotation of the molecule) and hot-band transitions, often with significant bending excitation [52–54]. The transitions observed in emission often have an increased chance of misassignment and mislabeling. A significant hindrance in the utilization of hot emission spectra is that it is usually not possible to obtain line positions with the same accuracy as those coming from absorption spectra recorded at room temperature. This is due to the increased Doppler width of the transitions and, in the case of atmospheric pressure spectra such as those recorded in flames, significant pressure broadenings and pressure shifts. The extended linewidth and the high density of observable transitions also lead to a very large number of blended transitions, which places a further constraint on the accuracy with which the positions of the individual peaks can be determined.

The emission spectrum recorded in Gießen and reported in Fig. 1 has several outstanding features: constant temperature of the hot molecular gas, low gas pressure (less than 20 mbar), reproducible emission line intensities with an accuracy usually better than 10%, almost fully resolvable spectral features (after the final deconvolution analysis), and high signal to noise ratio, up to 10000, due to the very low level of the modulated and not modulated background radiation. The simultaneous fulfillment of these characteristics and the use of a special emission spectrum analysis program are the strengths of the experimental apparatus developed in Gießen. These important characteristics allow us to extract accurate line positions and intensities from up to 2000 K hot emission spectra in general and improve the MARVEL list of energy levels for $H_2{}^{16}O$ in particular.

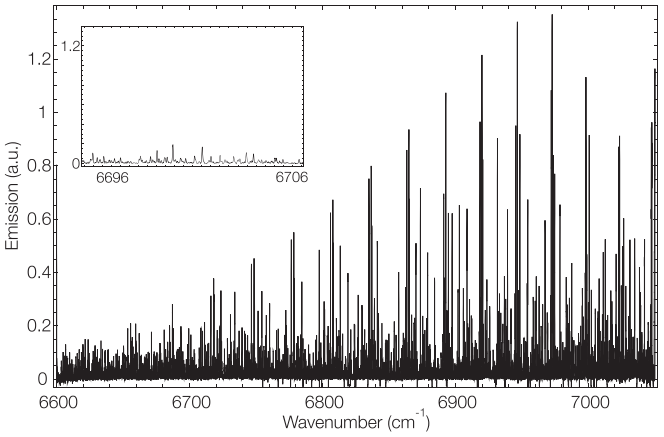

Fig. 1. Overview of the measured $H_2{}^{16}O$ emission spectrum. a.u. = arbitrary unit. The inset shows a narrow portion of the spectrum, all of the small features correspond to an emission peak. Due to the high signal to noise ratio, the noise level is smaller than the smallest feature one can see on these figures.

In this work we apply MARVEL energy levels [4,5], emission line intensities coming from the so-called BT2 database [55], and a computerized search algorithm to analyze a high-resolution emission spectrum, taken in Gießen at 1943 K, of the main water isotopologue, $H_2{}^{16}O$. It is our hope that the present study not only provides important new transition and energy-level data but also improves upon the methodology how high-resolution emission spectra of stable molecules are analyzed and assigned.

2. The MARVEL/BT2 (MB) peak list

Due to the assumed simplicity of the water molecule, it has been a favorite subject of variational nuclear motion computations [13,27,55–65]. As a result of considerable advancement in the field of computational quantum chemistry [26], systematic and mostly automated comparisons between the results of state-of-the-art variational nuclear motion computations and experiment are possible and they prove to be highly instructive.

In this study the BT2 line list [55] has been used; this line list was computed using a spectroscopically determined PES [59], an *ab initio* DMS [58], and the DVR3D [66] nuclear-motion program suite. A BT2 transition list was generated in the wavenumber range of the experiment, containing the complete set of transitions likely to be observed in the emission spectrum of Fig. 1. The emission intensities are extremely important when assigning measured emission spectra. The BT2 line list contains Einstein A_{if} coefficients for each transition; these Einstein-A coefficients have been used to compute the emission spectrum at 1943 K.

Measured spectra of $H_2{}^{16}O$ vapor are basically a superposition of two separate spectra, those of *ortho*-$H_2{}^{16}O$ and *para*-$H_2{}^{16}O$. The strongly forbidden transitions between the two nuclear-spin isomers have never been observed [67]. In the language of network theory [20,68], the transitions present in the spectra of $H_2{}^{16}O$ are part of two rooted components, *o*-$H_2{}^{16}O$ and *p*-$H_2{}^{16}O$.

For consistency and to maintain a single set of uniform labels for all levels, we chose to label rovibrational states and transitions following the recommendations of Tennyson et al. [4]. Thus, vibrations are labeled employing the usual normal-mode notation, $(v_1\, v_2\, v_3)$, while for the rotations we use the standard asymmetric-top quantum numbers $[J K_a K_c]$ or $J_{K_a K_c}$. Driven by the required uniqueness of the labels, the rotation-vibration levels of $H_2{}^{16}O$ are identified in this study by altogether six labels: $(v_1\, v_2\, v_3)$ $[J K_a K_c]$. The individual labels of the rovibrational states established by Tennyson et al. [4] were utilized unchanged.

After carefully matching the BT2 indices of the transition list and the labels of the MARVEL energy levels, pairs of experimental transition wavenumbers and experimental-quality intensities are obtained. We used this combined MARVEL/BT2 (henceforth MB) line list during the analysis of the high-resolution emission spectrum recorded.

3. Experimental details

The emission experiment is described in detail in a previous paper [69], which the reader is referred to for details. Thus, only a brief description of the experimental setup is given here.

The emission spectrum was recorded by replacing the spectrometer's near infrared source with a hot Al_2O_3 cell. The cell was fitted with CaF_2 windows and filled with 14.6 mbar of water vapor. The spectrum was recorded using an InSb quantum detector. The emitted radiation was focused by the transfer optics and an iris was used to block out the black-body radiation emitted from the inner surface of the emission cell. The experimental apparatus was optimized to reduce the shot noise present in the emission spectrum by eliminating the photons not emitted by the water molecules. The windows and the ends of the cell were kept at room temperature using water-cooled collars. To minimize the self-absorption and temperature inhomogeneity effects on the emission line shapes the length of the cell outside the oven was only 120 mm. A power spectrum from 1700 two-sided interferograms has been recorded with a resolution corresponding to 0.05 cm^{-1} full width at half height of the instrumental lineshape. A background spectrum recorded with the empty cell was used to extract the residual Planck emission background. The single-beam spectrum had a few absorption lines, these lines show up in the corrected emission spectrum as negative spectral features.

Fig. 1 shows an overview of the background-corrected emission spectrum. The most intense line in the spectrum, at about 6973 cm^{-1} corresponds to the following *ortho–para* pair of the (1 0 1) ← (0 0 0) excitation: $11_{1,11} - 12_{1,12}$ and $11_{0,11} - 12_{0,12}$ at 6972.7479 and 6972.7410 cm^{-1} respectively. There are several very intense lines, forming part of the fairly regular (1 0 1) ← (0 0 0) progression, on the left and right of the 6973 cm^{-1} peak. These transitions are characterized by the following changes in the rotational quantum numbers: $(J-1)_{0,J-1} - J_{0,J}$ and $(J-1)_{1,J-1} - J_{1,J}$. The separation of these lines is approximately 25–32 cm^{-1} the positions of the *ortho* lines are {6998.17, 6972.75, 6946.58, 6919.95, 6892.74, 6864.98, 6836.68, 6807.84, 6778.46, 6748.56, 6718.18, 6687.15, 6655.72, 6623.76} cm^{-1} for $J = 11 - 24$. The splittings of the *ortho–para* pairs are small, 0.0704 cm^{-1} for $J = 11$ and 0.0004 cm^{-1} for $J = 22$. Other nice and clear (1 0 1) ← (0 0 0) progressions can also be found in the spectrum, with very regular differences but considerably larger *ortho–para* separations (in line with expectation). These transitions are characterized by the following quantum number changes: $(J-1)_{1,J-2} - J_{1,J-1}$, $(J-1)_{2,J-2} - J_{2,J-1}$, $(J-1)_{2,J-3} - J_{2,J-2}$, and $(J-1)_{3,J-3} - J_{3,J-3}$. As expected, J varies between 8 and 16 for these transitions.

We used the MB peak list to calibrate the line positions and the intensities of the emission lines. Fig. 2 shows the differences between a set of 53 selected MARVEL transitions and the corresponding experimental line positions. The mean measurement uncertainty for these peaks in the MARVEL database is 0.002 cm^{-1}. The set includes peaks with relatively low as well as high intensity and peak positions determined during the deconvolution procedure from overlapping peaks. During the wavenumber calibration we assumed that due to the use of the MARVEL protocol the calculated transition wavenumbers are free from calibration errors. From Fig. 2 we can deduce an upper limit for the accuracy of the measured line positions, 0.003 cm^{-1}.

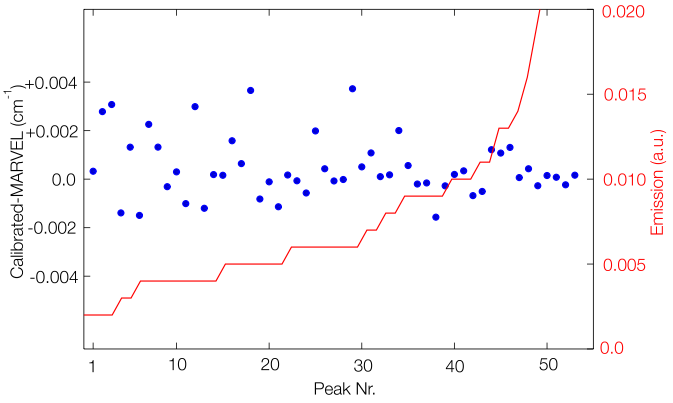

Fig. 2. Differences between the MARVEL and the calibrated experimental line positions for 53 selected peaks in the 6700–7000 cm^{-1} region. The intensity of the selected transitions is increasing from left to right from 0.002 to 0.039 a.u., where a.u. = arbitrary unit (see Fig. 1). The mean precision of the 53 MARVEL transition wavenumbers (determined in the MARVEL analysis) is 0.002 cm^{-1}.

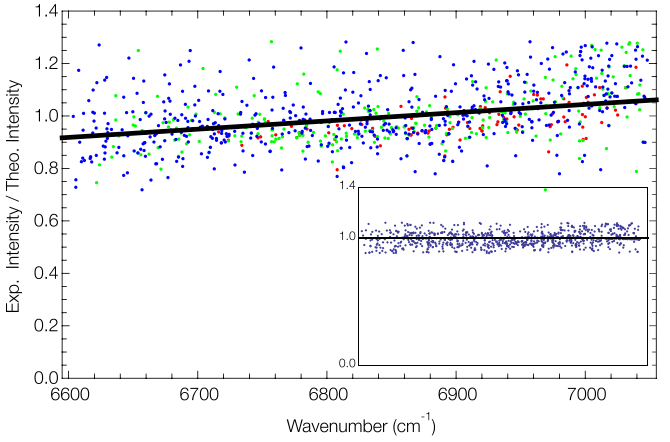

Fig. 3. Intensity calibration plot of the emission spectrum using the 200 most intense peaks. As expected, the intensity calibration curve is a simple linear curve. The inset shows the plot of the final intensity-calibrated SyMath lineshape database, where the number of low-intensity peaks included in the deconvolution was significantly increased. The measured line intensity is in outstanding agreement with the first-principles BT2 results.

Fig. 3 shows the intensity calibration plot using the 200 most intense unsaturated peaks showing no self-absorption effects. Clearly, the measured line intensities are in excellent agreement with the first-principles BT2 results, see, in particular, the inset of Fig. 3. Thus, it is expected that almost all computed intensities should have a discrepancy less than 25% when compared to the present experimental peak intensities.

The SyMath [69] spectrum deconvolution program was used to extract the measured line positions and relative intensities. First, an initial guess of the line positions and intensities have been calculated using SyMath's second-derivative peak-finding routine. Fixing the line widths to an average value an initial SyMath lineshape database was set up using Doppler lineshapes. In the second step the automated fit routine was used to fit the positions and intensities. In the third, visual-inspection step the peak list was further improved by inserting or deleting peaks manually. This procedure resulted in the starting peak list we used during the analysis of the measured emission spectrum.

The deconvolution procedure described by Mellau et al. [69] in detail is based on the simultaneous, step-by-step determination of the spectroscopic parameters of an effective Hamiltonian and of the corresponding deconvoluted peak list. The predictions, within experimental accuracy, of the positions and intensities for blended

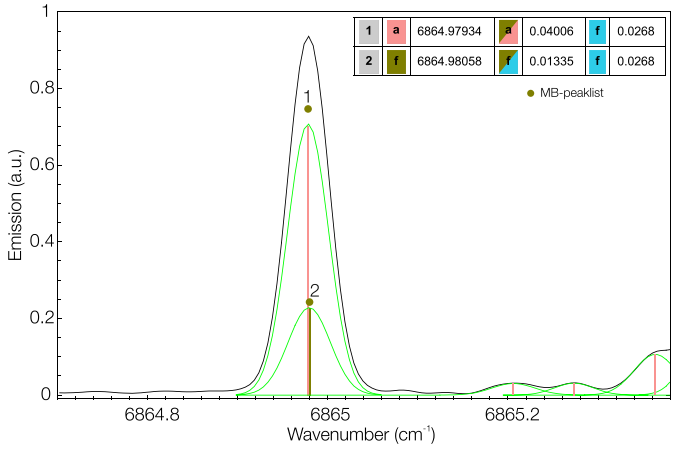

Fig. 4. A well-resolved, high-intensity line in the experimental emission spectrum of $H_2{}^{16}O$. The line consists of two nearby peaks with similar intensities. If the position and the intensity of one of the lines is fixed during the lineshape analysis, the experimental line position of the second line agrees with the transition wavenumber calculated using the MARVEL experimental energy levels within 0.001 cm^{-1}. There is also an excellent agreement between the measured relative intensities and the first-principles computed intensities.

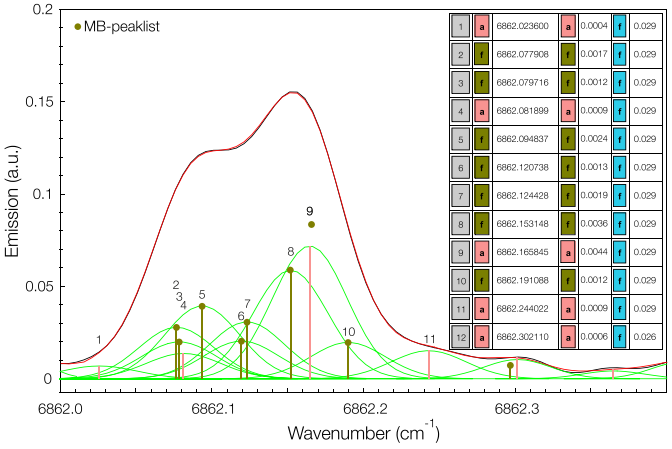

Fig. 6. Strongly overlapping peaks in the emission spectrum of $H_2{}^{16}O$, resolved with the help of the MB peak list. The red curve is the sum of the green single line shape curves and it is in excellent agreement with the black measured spectrum. (For interpretation of the references to colour in this figure legend, the reader is referred to the web version of this article.)

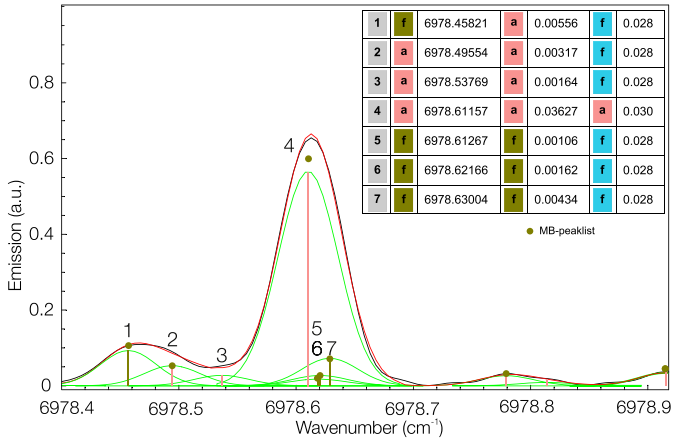

Fig. 5. An emission line of $H_2{}^{16}O$ with significant disturbers in the neighborhood of the main peak. To obtain an accurate line position a deconvolution analysis of the spectral feature is needed. Including the three small lines, 5, 6, and 7, in the deconvolution the position of the strong line changes from 6978.6128 cm^{-1} to 6978.6116 cm^{-1}, the transition wavenumber calculated using MARVEL levels is 6978.6118 cm^{-1}.

lines is integrated step by step during the deconvolution analysis of the overlapping peaks. The result is a dynamic peak list where the lineshape parameters are improved as the analysis is progressing. The final peak list is found in fact at the end when the assignment of the spectrum is completed.

We used the MB peak list for a deconvolution procedure similar to the one described by Mellau et al. [69]: using the SyMath program the line position and intensity information from the MB peak list was integrated into the deconvolution of the emission spectrum. The heart of this type of analysis is the simultaneous refinement of line positions and intensities. Thus, one needs an accurate theoretical prediction for the intensity of the lines. For the analysis of the HCN lines [69], for example, effective formulas have been used to fit the band intensities. Here, on the other hand, we employ the first-principles BT2 intensities.

Figs. 4–6 contain edited screen shots from the SyMath analysis program. These figures show the measured emission spectrum, the Doppler line shapes of the individual emission peaks, and the simulated spectrum as the sum of the individual Doppler-broadened lines. The inset tables of these figures are edited screen shots of the SyMath user interface. For each peak the user interface allows to select which lineshape parameter should be fixed (f) or adjusted (a) and, if necessary, set any parameters to predefined values. The tables of Figs. 4–6 show pairs of colored f/a switch buttons and selected parameter values: the first pair of columns corresponds to the line position parameter of the Doppler line shape, while the second and third pairs give line intensity and line width parameters, respectively. Occasionally an additional choice (and color code) has also been introduced, marking the lineshape parameters fixed during the analysis of the calculated values of the MB peak list. Note that line width parameters, with a few exceptions, have been fixed during the final spectrum analysis (see the insets of Figs. 4–6). Nevertheless, in the majority of the cases they have been adjusted in the first step of the analysis and then these values have been employed during the final analysis step.

Fig. 4 shows an intense line, part of the (1 0 1) ← (0 0 0) progression with $J = 16$ (*vide supra*), with no major other overlapping lines. In the MB peak list this peak corresponds to two nearby, strong *ortho*- and *para*-$H_2{}^{16}O$ lines. The MB peak list occasionally indicated that a measured line is a superposition of two "nearly degenerate" transitions. In these cases we simulated, during the deconvolution analysis, the nearly degenerate *ortho–para* pairs according to the predicted relative intensities. For the spectral feature of Fig. 4 the analysis progressed by fixing the line position of one of the peaks to the value predicted by the MB peak list. The intensity of this peak was fixed to a value so that after the deconvolution procedure the relative intensities of the two overlapping peaks match the 1:3 ratio of the intensities given by the MB peak list. In particular, according to the MB peak list there is an *ortho* line at 6864.9790 cm^{-1} with a peak intensity of 0.043, while the corresponding *para* line is at 6864.9794 cm^{-1} with an intensity of 0.014. Fixing the *para* line position to the MB peak-list value and the intensity to 0.013, the deconvolution gives, for the experimental *ortho* peak, 6864.9794 cm^{-1} for the position and 0.040 for the intensity. This simple analysis step often allows to map, one by one, the experimental peak list to the MB peak list. In many other cases an alternative analysis was made: first, a single peak was adjusted and then, in a second step, two peaks have been defined with a common line position and an exact 1:3 intensity ratio, with the intensity based on the parameters determined during the first step.

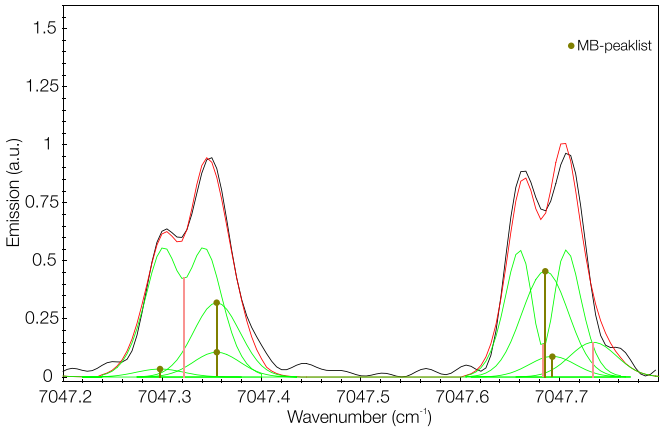

Fig. 7. Two examples of measured emission lines incorporating self-absorption features. We simulated the self-absorption lines with a combined emission and absorption line shape with two different line widths and intensities but a common line position.

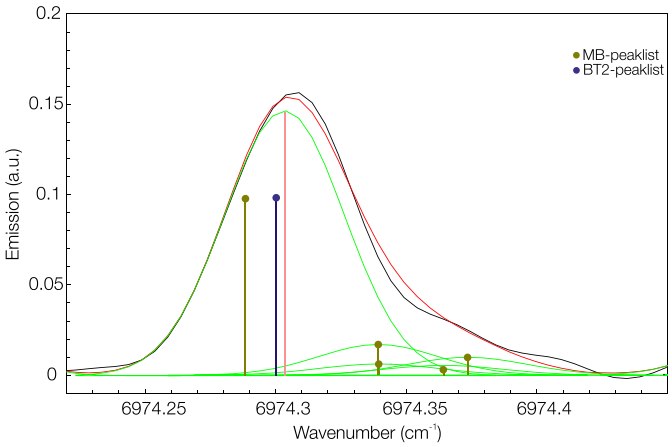

Fig. 8. An example when some of the MB peak positions do not coincide, within experimental accuracy, with the emission lines that make up the observed spectral features. This happens for transitions for which the uncertainty of the corresponding MARVEL energy levels is as large as 0.02 cm^{-1}. This slightly off-centered MARVEL prediction improves after including the newly measured experimental peak in the MARVEL analysis.

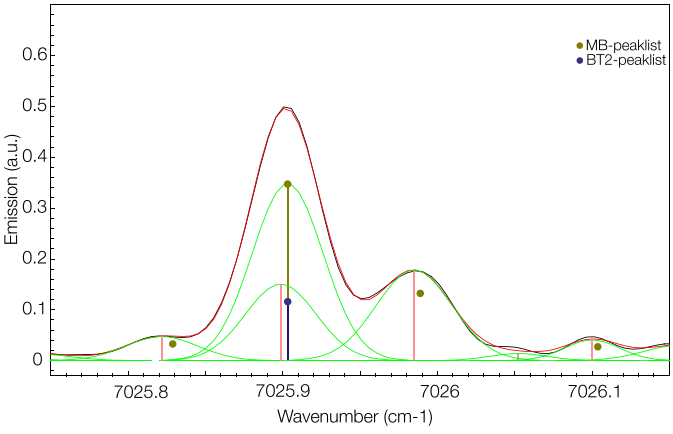

Fig. 9. Due to the accurate intensity match between theory and experiment, it is possible to detect and assign transitions not present in the MB peak list even in the case where the new transition overlaps with other peaks. This peak corresponds to a transition between states where either the lower and/or the upper energy levels are missing from the MARVEL list of rovibrational energies. There is a first-principles transition corresponding to this line.

Fig. 5 shows a slightly more complicated case: a measured line overlaps with some peaks of much smaller intensity. In general, the accuracy of the deconvolution analysis depends on the additional knowledge we can include in the analysis regarding the form of the lineshape, the number of overlapping peaks, and the position and intensity of some of the overlapping peaks. The small peaks in Fig. 5 disturb the position and the intensity of the main peak; to obtain an accurate line position and intensity a deconvolution analysis of the spectral feature is needed [69]. Including the small lines 5, 6, and 7 in the deconvolution, the position of the main line changes from 6978.6128 cm^{-1} to 6978.6116 cm^{-1}; the transition wavenumber calculated using MARVEL energy levels is 6978.6118 cm^{-1}.

In some cases, especially for peaks with low intensity, the lines in the emission spectrum are composed of two or often considerably more peaks, resulting in various spectral features with relatively large effective widths. For example, for the spectral feature shown in Fig. 5 the width is 0.13 cm^{-1}. The red curve of Fig. 6 is the sum of the green single line shape curves and is in excellent agreement with the black curve of the measured spectrum. Even though the majority of the lineshape parameters are fixed to the values of the MB peak list, this analysis gives us important experimental results: in the process of the labeling we know that in this wavenumber region there are no peaks with an intensity greater than 0.0009 and we have some overall experimental information regarding the intensity of the measured peaks.

The hot water emission spectrum investigated contains self-absorption spectral features, as well (an example is given in Fig. 7). `SyMath` allows to assign a different lineshape to each peak present in the deconvolution analysis. We simulated the self-absorption lines with a combined emission and absorption line shape with two different line widths and intensities, but a common line position. In the majority of the cases, we fixed the intensity of the emission part to the value computed for a pure emission case. It is somewhat uncertain whether such a spectral feature in the emission spectrum should be assigned to two separate, nearby peaks or to a single self-absorption feature. For the spectrum studied in this work the position of all self-absorption features have been predicted by MARVEL energies and thus simulated by a single peak.

Some MB peaks do not coincide, within experimental accuracy, with the emission lines that make up the observed spectral features. This happens especially for transitions for which the accuracy of the corresponding MARVEL energy levels is only 0.02 cm^{-1}, an uncertainty much larger than the usual uncertainty of the empirical MARVEL energy levels. Fig. 8 shows such a case, where using the deconvolution procedure we can determine accurate peak positions. Including these new transitions in the MARVEL analysis protocol results in energy levels with significantly improved accuracy and precision.

Due to the accurate intensity match between theory and experiment it is possible to detect and assign transitions not present in the MB peak list even when the new transition overlaps with many other peaks. Fig. 9 shows emission peaks at 7025.9 cm^{-1}, where the MB peak list does not predict one of the experimental peaks. This peak corresponds to a transition between states where either the lower and/or the upper energy levels are missing from the MARVEL list of rovibrational energies. The experimental peak at 7025.903 cm^{-1} has no MARVEL counterpart and thus leads to a new energy level. Note also that there is a first-principles line with a suitable label for the peaks shown in Figs. 8 and 9.

4. Assignment of the spectrum

4.1. Mapping experimental and MB peaks

A computerized search algorithm was developed to map the measured emission peaks to the MB peak list as well as to first-principles BT2 transitions if a peak was found to be missing from the MB peak list. The mapping algorithm uses both wavenumber and intensity matching criteria: for each experimental peak, starting with the most intense one, the algorithm searches for unassigned transitions that simultaneously fulfill the 0.006 cm^{-1} line position and 40% intensity match criteria. Based on the line position and intensity calibration (Figs. 2 and 3), these conservative choices appeared to be reasonable for an automated search. When more than one transition matches the criteria, the "closest one" in intensity and position is chosen, with priority given to the position match.

The search algorithm takes into account that in some cases, in particular for overlapping *ortho* and *para* transitions, only a single peak is present in the measured peak list (not all such peaks have been replaced by two peaks with corresponding relative intensities during the deconvolution procedure). In such cases the experimental peak may be at a slightly shifted wavenumber from those of the true *ortho* and *para* transitions and its intensity differs from the computed values. We calculated a virtual peak list with a single position and intensity entry for the cases with overlapping *ortho* and *para* peaks. The assignment algorithm checked this *ortho–para* convoluted peak list and in many cases proposed reasonable assignments, especially for the low-intensity peaks.

4.2. Search for unknown energy levels

The MARVEL database of $H_2{}^{16}O$ [4] is the largest available empirical rovibrational eigenenergy database for this molecule. The accuracy and completeness of this database allowed us to develop a computerized algorithm to detect new experimental energy levels based only on MARVEL transitions and first-principles BT2 line intensities, without the use of an effective Hamiltonian. We used this algorithm to map emission peaks to BT2 transitions for which only the lower MARVEL level is known.

The first step in the assignment is the selection of an unassigned experimental peak with approximately the same intensity as that of the BT2 line. Choosing the proper "free" experimental peak is not a straightforward task, there are at least three aspects that make this step difficult. First, the majority of the unassigned peaks has low intensity and the density of such peaks is high. Second, at low intensity there is a significant blending in the experimental spectrum, the quality of the deconvolution decreases with decreasing line intensity. Third, the BT2 lines can be shifted by as much as 0.5 cm^{-1} from the experimental lines. Therefore, sometimes there remains an ambiguity in assigning an experimental peak to a predicted BT2 line.

To at least partially circumvent these difficulties, we attempted to confirm the assignment of the upper state by looking for other BT2 transitions with the selected upper state in the measured 6600 to 7050 cm^{-1} region. As a further constraint, during this procedure we chose those experimental peaks which shifted from the respective BT2 transitions by approximately the same amount. After finding the proper experimental peak, we made an approximation for the energy of the new upper state: the wavenumber of the experimental peak plus the MARVEL energy of the lower level.

4.3. Labels

As a final step, for each detected transition with an unknown upper state the vibrational and rotational labels (only J is known from BT2) have to be determined. The labels were generated based on the following considerations:

- A list of possible vibrational quantum numbers $(v_1\, v_2\, v_3)$ can be generated by using BT2 vibrational energy levels and the rotational energy value of the given $[J\, K_a\, K_c]$ in the ground vibrational state. The sum of these two energies must fall into a predefined range in order to consider the label further.
- The rotational quantum numbers $[JK_aK_c]$ must fulfill the following selection rules: $\Delta J = 0, \pm 1$; $\Delta K_a = 0, \pm 1, \pm 3$, as well as the parity selection rule.
- Possible upper levels are constructed from the possible vibrational band origins (VBO) and possible rotational upper levels with the following constraint [4]: $(-1)^{(v_3^{up}+K_a^{up}+K_c^{up})} = (-1)^{(v_3^{low}+K_a^{low}+K_c^{low})}$.
- Check the MARVEL dataset and rule out those possible upper levels which already exist in MARVEL.
- Delete those levels which do not satisfy the assumption that the energy must increase with an increase in K_a.

With the help of the above considerations we usually obtained 5–15 possible labels. To facilitate selection of the correct one we did the following:

- We have developed a "hole-finding" algorithm, which searches for "holes" in the MARVEL energy-level list. Then we investigated which predicted energy value fits the hole the best. To find this "hole" we apply two linear approximations. We suppose that there are linear relationships between (a) K_a and the MARVEL energy values within the same VBO; and (b) the VBOs and the MARVEL energy values for a given rotational state. Fig. 10 shows this linear relationship between K_a and the MARVEL energies for the (3 0 0) vibrational band. The red dot represents an unknown energy level. Fig. 11 shows the $[JK_aK_c]$ = [16 0 16] rotational energies for different vibrational states. As can be seen, there are two "holes", for the vibrational states (1 3 0) and (2 1 0). Although these approximations are rather inaccurate (50–200 cm^{-1}) in their absolute energy values, due to the clear observed tendencies they can be used to confirm labels for so far unknown rovibrational states.

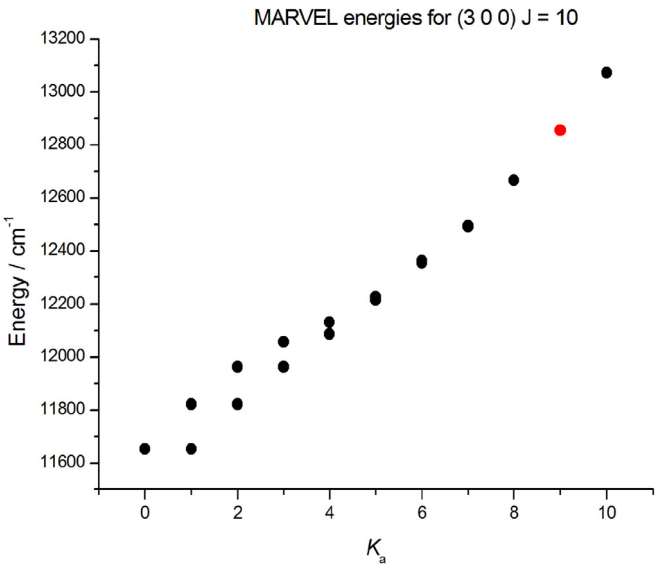

Fig. 10. Nearly linear relationship between the K_a quantum number and the MARVEL energies for the (3 0 0) vibrational band, shown by the black dots. The red dot shows a missing energy level. (For interpretation of the references to colour in this figure legend, the reader is referred to the web version of this article.)

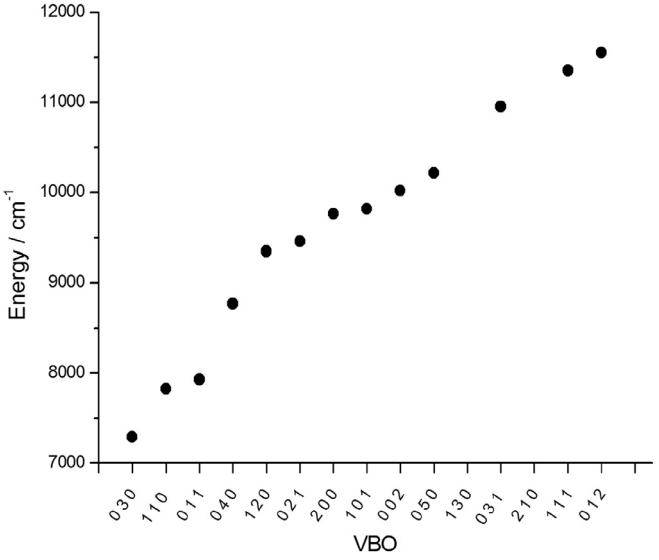

Fig. 11. The rotational energies of $[JK_aK_c] = [16\ 0\ 16]$ for different vibrational states $(v_1\ v_2\ v_3)$.

- In some cases selecting the correct quantum numbers can be based on pairing a MARVEL energy (if it exists, *e.g.*, the pair of (2 0 0) [12 11 1] is (2 0 0) [12 11 *x*]), and only one (or none) can be found in MARVEL. If this energy pair is close to the predicted energy, it is the best label for the new level.
- To some extent, our decisions have been based on the investigation of other (new) transitions the new energy level participates in. We employed a scoring scheme based on how these transitions obey selection rules. Those transitions are considered best which obey strict selection rules, $\Delta K_a = 0$, 1, and 3; a penalty score was employed for those transitions which do not obey them.

The difficulty with all these rules, and possible assignments, is that in emission spectra the simple selection rules stated are not that strict. Certain other transitions can happen; naturally, with lower probability than $\Delta K_a = 0$, 1, and 3. However, we considered the label of a new energy level to be more viable if the corresponding transitions are better in the sense of obeying simpler selection rules.

Unfortunately, none of the above criteria is stronger than the other. There is no clear rule about their order, often times one must rely on "intuition". Careful, one-by-one investigation of the above criteria was needed for finding out the correct labels for the new energy levels. It is also important to note that not all of the above criteria can be employed in each and every case, due to the lack of suitable MARVEL energy levels.

4.4. New transitions corresponding to old energy levels

The MB peak list contains more than 96 000 lines in the spectral region of the emission spectrum with a relative intensity larger than 0.0002. During the last SyMath refinement, we retrieved from the emission spectrum recorded about 6700 peaks. In this work we assigned close to 3700 of these peaks. All of the measured peaks with a relative intensity larger than 0.005 and not suffering from self-absorption have been assigned.

In 73% of the cases an automatic assignment was feasible as the measured peaks do coincide, within experimental uncertainty, with transitions predicted using MARVEL eigenenergies. In the rest of the cases, where the automatic assignment procedure was not able to assign the emission peaks, it was still possible to assign the peaks by a careful visual inspection.

Finally, note that a few relatively large peaks with an intensity of 0.0005–0.001 have been assigned to OH transitions.

4.5. Correcting the MARVEL dataset

11 of the predicted MB peaks proved to be outliers when compared to the present observed spectrum. Therefore, the corresponding information was deleted from the MARVEL dataset. These MB peaks originate from energy levels obtained from poorly defined experimental transitions, they mostly come from previous emission studies. The following previously reported [4] energy levels had to be deleted based on the present emission measurement: (1 0 1)[15 5 10], (1 0 1)[15 10 6], (0 0 2)[16 7 10], and (2 0 0)[15 6 10].

4.6. Transitions leading to new energy levels

We found about 100 relatively intense peaks that were missing from the MB peak list. These are the lines which would define new experimental energy levels if successfully assigned. In fact, we determined 23 new rovibrational levels of $H_2{}^{16}O$ and characterized them in this work (see the E_{up} entries of Table 1). A first-principles-based assignment procedure similar to that described above was employed to assign these peaks.

The first set of assigned peaks have known experimental lower states and the upper level is participating in at least two transitions (see Table 1). Based on these measured transitions, we determined the eigenenergy of 10 new rovibrational states. In most cases both the BT2 and the measured intensities of the second transition confirming the assignment are rather low. It is then not straightforward to find the corresponding experimental peak.

The further new rovibrational levels reported in Table 1 have been determined based on only one observed transition. We are confident that the labels determined for this second set are correct as they correspond to close-lying *ortho–para* pairs. Close-lying *Ortho–para* pairs formed a special case during our search for new energy levels: if the *ortho* part of a pair is already assigned, we can detect the peak corresponding to the *para* transition pair based on the position and the well-defined difference between the measured and the predicted intensity. In these cases choosing the correct label for the assigned peak is straightforward.

A special case of *ortho–para* pairs is where the *ortho* part of the pair remained unassigned in the automated procedure due to a MARVEL energy level with insufficient accuracy. In such cases a careful visual investigation of the spectrum and the predicted MARVEL and BT2 wavenumbers and labels allows the assign ment of the two peaks of the *ortho–para* pair. In such cases we corrected the "bad" MARVEL entry, shifted it to the correct value, and then the corresponding *para* part was assigned.

It is of interest to note here that in the transitions leading to newly assigned energy levels only the following lower vibrational states are involved: (0 0 0), (1 0 0), (0 1 0), and (0 0 1). The upper vibrational states show only a slightly larger variety: (1 0 1), (2 0 0), (1 1 1), (2 1 0), (3 0 0), and (2 0 1). The J rotational quantum number is also constrained to a relatively narrow range, $10 \le J \le 16$.

5. Summary and conclusions

Investigation of an emission spectrum recorded at high resolution at 1943 K in the wavenumber range of 6600–7050 cm^{-1} yielded a large number of transitions not available from previous studies and a small number of new rovibrational energy levels.

The emission spectrum corresponds to more than 6700 identified peaks, more than half of them (about 3700) could be assigned,

Table 1
New rovibrational energy levels (E_{up}) of $H_2{}^{16}O$ determined by newly measured emission lines ($\tilde{\nu}$) and the corresponding assignments.

$\tilde{\nu}$/cm^{-1}	E_{up}/cm^{-1}	$(v_1v_2v_3)_{up}$	$[JK_aK_c]_{up}$	E_{low}/cm^{-1}	$(v_1v_2v_3)_{low}$	$[JK_aK_c]_{low}$	p/o	$10^3 I_{rel}^{BT2}$	$10^3 I_{rel}^{meas}$
6781.986(6)	9734.37(1)	(2 0 0)	15 2 14	2952.387(4)	(0 0 0)	16 1 15	p	35	34
6861.790(10)		(2 0 0)	15 2 14	2872.580(2)	(0 0 0)	15 3 13	p	7	8
7025.903(6)	10792.2892(6)	(1 0 1)	12 12 1	3766.387(8)	(0 0 0)	12 12 0	p	113	117
6704.309(6)		(1 0 1)	12 12 1	4087.981(4)	(0 0 0)	13 12 2	p	7	7
6650.015(6)	11077.243(6)	(1 0 1)	15 9 6	4427.228(5)	(0 0 0)	16 9 7	p	19	29
7031.959(6)		(1 0 1)	15 9 6	4045.286(2)	(0 0 0)	15 9 7	p	26	41
7007.273(6)	11438.911(6)	(1 0 1)	14 12 3	4431.638(2)	(0 0 0)	14 12 2	p	50	54
6998.679(6)	11767.909(6)	(1 1 1)	11 10 1	4769.233(2)	(0 1 0)	11 10 2	p	44	66[a]
6703.766(6)		(1 1 1)	11 10 1	5064.143(3)	(0 1 0)	12 10 2	p	8	6[a]
6659.366(6)	11868.371(6)	(1 1 1)	13 8 5	5208.992(2)	(0 1 0)	14 8 6	p	17	12
6996.409(6)		(1 1 1)	13 8 5	4871.949(2)	(0 1 0)	13 8 6	p	20	27
6964.433(6)	11931.476(6)	(1 0 1)	14 14 1	4967.043(2)	(0 0 0)	14 14 0	p	49	50
6613.342(6)	11955.694(6)	(2 1 0)	14 6 9	5342.347(2)	(0 1 0)	15 7 8	o	48	33
6975.479(6)		(2 1 0)	14 6 9	4980.223(2)	(0 1 0)	14 7 8	o	24	24
6974.305(6)	12040.534(6)	(1 0 1)	15 13 2	5066.230(2)	(0 0 0)	15 13 3	p	34	35
6991.493(6)	12055.635(6)	(1 1 1)	12 10 3	5064.143(2)	(0 1 0)	12 10 2	p	30	30
6674.084(6)		(1 1 1)	12 10 3	5381.553(3)	(0 1 0)	13 10 4	p	9	12
6953.249(6)	12292.921(6)	(1 0 1)	15 14 1	5339.673(2)	(0 0 0)	15 14 2	p	29	27[a]
6931.151(6)	12545.239(6)	(1 0 1)	15 15 0	5614.090(2)	(0 0 0)	15 15 1	p	34	31
6948.047(6)	12560.540(6)	(1 1 1)	12 12 1	5612.494(3)	(0 1 0)	12 12 0	p	31	32
6941.911(6)	12675.065(6)	(1 0 1)	16 14 2	5733.155(2)	(0 0 0)	16 14 3	o	49	49[b]
6941.911(6)	12675.065(6)	(1 0 1)	16 14 3	5733.155(2)	(0 0 0)	16 14 2	p	16	16[a]
6716.703(6)	12856.025(6)	(3 0 0)	10 9 2	6139.323(2)	(0 0 1)	10 9 1	o	34	34[b]
6990.421(6)		(3 0 0)	10 9 2	5865.604(2)	(1 0 0)	10 8 3	o	6	14[b]
6716.703(6)	12856.025(5)	(3 0 0)	10 9 1	6139.323(2)	(0 0 1)	10 9 2	p	11	11[a]
6990.421(6)		(3 0 0)	10 9 1	5865.604(2)	(1 0 0)	10 8 2	p	1	5[a]
6928.998(6)	13209.560(6)	(1 1 1)	14 12 2	6280.563(3)	(0 1 0)	14 12 3	o	44	45[b]
6928.998(6)	13209.560(6)	(1 1 1)	14 12 3	6280.563(3)	(0 1 0)	14 12 2	p	11	15[a]
6698.765(6)	13393.335(6)	(3 0 0)	12 9 4	6694.579(2)	(0 0 1)	12 9 3	o	18	19[b]
6987.805(6)		(3 0 0)	12 9 4	6405.517(2)	(0 0 1)	11 9 3	o	8	18
6976.049(6)		(3 0 0)	12 9 4	6417.296(2)	(1 0 0)	12 8 5	o	8	17
6698.765(6)	13393.338(6)	(3 0 0)	12 9 3	6694.578(2)	(0 0 1)	12 9 4	p	6	6[a]
6767.947(6)	13553.544(6)	(2 0 1)	11 11 0	6785.599(3)	(1 0 0)	11 11 1	p	20	26
6751.835(6)	12164.836(6)	(0 5 1)	9 0 9	5413.003(2)	(0 3 0)	8 0 8	p	11	11

[a] Adjusted measured intensity, obtained after subtracting the intensity corresponding to the coincident *ortho* line.
[b] Adjusted measured intensity, obtained after subtracting the intensity corresponding to the coincident *para* line.

yielding close to 4100 assignments, employing an elaborate iterative procedure developed during the present study. The assignment procedure builds heavily on previously determined empirical (MARVEL) rovibrational energy levels and accurate first-principles intensities. Both the transitions obtained from the experimental energy levels and the intensities proved to be highly useful during the assignment of the measured emission spectrum. For example, the accuracy of the computed intensities allowed the identification of coincident *ortho*- and *para*-$H_2{}^{16}O$ transitions.

There are about 4500 energy levels taking part in the measured and assigned transitions, about 2800 of these are upper energy levels. There are more than 1300 transitions observed for the first time which connect previously measured energy levels. These transitions define about 1300 new fundamental cycles of the experimental spectroscopic network of $H_2{}^{16}O$, considerably enhancing any MARVEL-type analysis of the available experimental information. In fact, due to the inclusion of the new transitions in the MARVEL analysis the average accuracy of the energy levels taking part in the newly measured transitions decreased from 0.0047 to 0.0036 cm^{-1}, a significant improvement of the MARVEL database of $H_2{}^{16}O$ transitions.

The measured peak list of the present investigation and the assigned transitions are available as Supplementary Information to this paper. This information is also part of the ReSpecTh information system, which can be accessed via http://www.respecth.hu/.

Acknowledgments

This work received support from NKFIH (grant K119658). The COST action CM1405 (MOLIM: Molecules in Motion) is acknowledged for its support of the collaborative part of this work.

Supplementary material

Supplementary material associated with this article can be found, in the online version, at 10.1016/j.jqsrt.2017.10.028.

References

[1] Bernath PF. The spectroscopy of water vapour: experiment, theory and applications. Phys Chem Chem Phys 2002;4:1501–9.
[2] Maksyutenko P, Grechko M, Rizzo TR, Boyarkin OV. State-resolved spectroscopy of high vibrational levels of water up to the dissociative continuum. Phil Trans Royal Soc London A 2012;370:2710–27.
[3] Polyansky OL, Zobov NF, Mizus II, Lodi L, Yurchenko SN, Tennyson J, et al. Global spectroscopy of the water monomer. Phil Trans Royal Soc London A 2012;370:2728–48.
[4] Tennyson J, Bernath PF, Brown LR, Campargue A, Császár AG, Daumont L, et al. IUPAC critical evaluation of the rotational-vibrational spectra of water vapor. part III. energy levels and transition wavenumbers for $H_2{}^{16}O$. J Quant Spectrosc Radiat Transfer 2013;117:29–58.
[5] Tennyson J, Bernath PF, Brown LR, Campargue A, Császár AG, Daumont L, et al. A database of water transitions from experiment and theory (IUPAC technical report). Pure Appl Chem 2014;86:71–83.
[6] Tennyson J, Bernath PF, Campargue A, Császár AG, Daumont L, Gamache RR, et al. Recommended isolated-line profile for representing high-resolution spectroscopic transitions (IUPAC technical report). Pure Appl Chem 2014;86:1931–43.
[7] Furtenbacher T, Szidarovszky T, Hruby J, Kyuberis AA, Zobov NF, Polyansky OL, et al. Definitive ideal-gas thermochemical functions of the $H_2{}^{16}O$ molecule. J Phys Chem Ref Data 2016;45. 043104.
[8] Zobov NF, Shirin SV, Polyansky OL, Tennyson J, Coheur P-F, Bernath PF, et al. Monodromy in the water molecules. Chem Phys Letts 2005;414:193–7.
[9] Császár AG, Allen WD, Schaefer III HF. In pursuit of the ab initio limit for conformational energy prototypes. J Chem Phys 1998;108:9751–64.
[10] Tarczay G, Császár AG, Klopper W, Szalay V, Allen WD, Schaefer III HF. The barrier to linearity of water. J Chem Phys 1999;110:11971–81.
[11] Valeev EF, Allen WD, Schaefer III HF, Császár AG. The second-order Moller–Plesset limit for the barrier to linearity of water. J Chem Phys 2001;114:2875–8.

[12] Maksyutenko P, Rizzo TR, Boyarkin OV. A direct measurement of the dissociation energy of water. J Chem Phys 2006;125. 181101.
[13] Zobov NF, Shirin SV, Lodi L, Silva BC, Tennyson J, Császár AG, et al. First-principles rotation-vibration spectrum of water above dissociation. Chem Phys Lett 2011;507:48–51.
[14] Szidarovszky T, Császár AG. Low-lying quasibound rovibrational states of $H_2{}^{16}O$. Mol Phys 2013;111:2131–46.
[15] Mellau GC. Complete experimental rovibrational eigenenergies of HNC up to 3743 cm^{-1} above the ground state. J Chem Phys 2010;133. 164303.
[16] Mellau GC. Complete experimental rovibrational eigenenergies of HCN up to 6880 cm^{-1} above the ground state. J Chem Phys 2011;134. 234303.
[17] Tennyson J, Bernath PF, L RB, Campargue A, Carleer MR, Császár AG, et al. Critical evaluation of the rotational-vibrational spectra of water vapor. Part I. Energy levels and transition wavenumbers for $H_2{}^{16}O$ and $H_2{}^{16}O$. J Quant Spectrosc Radiat Transfer 2009;110:573–96.
[18] Tennyson J, Bernath PF, Brown LR, Campargue A, Carleer MR, Császár AG, et al. Critical evaluation of the rotational-vibrational spectra of water vapor. Part II. Energy levels and transition wavenumbers for $HD^{16}o$, $HD^{17}o$, and $HD^{18}o$. J Quant Spectrosc Radiat Transfer 2010;110:2160–21841.
[19] Tennyson J, Bernath PF, Brown LR, Campargue A, Császár AG, Daumont L, et al. IUPAC critical evaluation of the rotational-vibrational spectra of water vapor. Part IV. Energy levels and transition wavenumbers for $d_2^{16}o$, $d_2^{17}o$ and $d_2^{18}o$. J Quant Spectrosc Rad Transfer 2014;142:93–108.
[20] Császár AG, Furtenbacher T, Árendás P. Small molecules – big data. J Phys Chem A 2016;120:8949–69.
[21] Császár AG, Furtenbacher T. Spectroscopic networks. J Mol Spectrosc 2011;266:99–103.
[22] Császár AG, Furtenbacher T, Czakó G, Mátyus E. An active database approach to complete spectra of small molecules. Ann Rep Comp Chem 2007;3:155–76.
[23] Furtenbacher T, Császár AG, Tennyson J. MARVEL: measured active rotational-vibrational energy levels. J Mol Spectrosc 2007;245:115–25.
[24] Furtenbacher T, Császár AG. On employing $H_2{}^{16}O$, $H_2{}^{17}O$, $H_2{}^{18}O$, and $D_2{}^{16}O$ lines as frequency standards in the 15 – 170 cm^{-1} window. J Quant Spectrosc Radiat Transfer 2008;109:1234–51.
[25] Furtenbacher T, Császár AG. MARVEL: measured active rotational-vibrational energy levels. II. Algorithmic improvements. J Quant Spectrosc Radiat Transfer 2012;113:929–35.
[26] Császár AG, Fábri C, Szidarovszky T, Mátyus E, Furtenbacher T, Czakó G. Fourth age of quantum chemistry: molecules in motion. Phys Chem Chem Phys 2012;13:1085–106.
[27] Polyansky OL, Császár AG, Shirin SV, Zobov NF, Barletta P, Tennyson J, Schwenke DW, Knowles PJ. High-accuracy ab initio rotation-vibration transitions for water. Science 2003;299:539–42.
[28] Tóbiás R, Furtenbacher T, Császár AG. Cycle basis to the rescue. J Quant Spectrosc Radiat Transfer 2017;203:557–64.
[29] Pine AS, Coulombe MJ, Camy-Peyret C, Flaud J-M. Atlas of the high-temperature water vapor spectrum in the 3000 to 4000 cm^{-1} region. J Phys Chem Ref Data 1983;12:413–65.
[30] Amano T, Scappini F. Millimeter-wave spectrum of rotationally excited H_2O. Chem Phys Lett 1991;182:93–5.
[31] Pearson JC, Anderson T, Herbst E, De Lucia FC, Helminger P. Millimeter- and submillimeter-wave spectrum of highly excited states of water. Astrophys J 1991;379:L41–3.
[32] Dana V, Mandin JY, Camy-Peyret C, Flaud J-M, Rothman LS. Rotational and vibrational dependences of collisional linewidths in the $n\nu_2 - (n-1)\nu_2$ hot bands of H_2O from fourier-transform flame spectra. Appl Opt 1992;31:1179–84.
[33] Dana V, Mandin JY, Camy-Peyret C, Flaud J-M, Chevillard JP, Hawkins RL, et al. Measurements of collisional linewidths in the ν_2 band of H_2O from fourier-transform flame spectra. Appl Opt 1992;31:1928–36.
[34] Mandin JY, Dana V, Camy-Peyret C, Flaud J-M. Collisional widths of pure rotational transitions of H_2O from fourier-transform flame spectra. J Mol Spectrosc 1992;152:179–84.
[35] Polyansky OL, Busler JR, Guo BJ, Zhang KQ, Bernath PF. The emission spectrum of hot water in the region between 370 and 930 cm^{-1}. J Mol Spectrosc 1996;176:305–15.
[36] Lanquetin R, Coudert LH, Camy-Peyret C. High-lying rotational levels of water: an analysis of the energy levels of the five first vibrational states. J Mol Spectrosc 2001;296:305–15.
[37] Coudert LH, Pirali O, Vervloet M, Lanquetin R, Camy-Peyret C. The eight first vibrational states of the water molecule: measurements and analysis. J Mol Spectrosc 2004;228:471–98.
[38] Camy-Peyret C, Flaud J-M, Maillard JP, Guelachvili G. Spectrum of water vapor between 8050 and 9370 cm^{-1}. Mol Phys 1977;33:1641–50.
[39] Polyansky OL, Tennyson J, Bernath PF. The spectrum of hot water: rotational transitions and difference bands in the (020), (100), and (001) vibrational states. J Molec Spectrosc 1997;186:213–21.
[40] Polyansky OL, Zobov NF, Viti S, Tennyson J, Bernath PF, Wallace L. High temperature rotational transitions of water in sunspot and laboratory spectra. J Mol Spectrosc 1997;186:422–47.
[41] Polyansky OL, Zobov NF, Tennyson J, Lotoski JA, Bernath PF. Hot bands of water in the ν_2 manifold up to $5\nu_2 - 4\nu_2$. J Mol Spectrosc 1997;184:35–50.
[42] Esplin MP, Wattson RB, Hoke LB, Rothman LS. High-temperature spectrum of H_2O in the 720–1400 cm^{-1} region. J Quant Spectrosc Radiat Transfer 1998;60:711–39.
[43] Zobov NF, Polyansky OL, Tennyson J, Lotoski JA, Colarusso P, Zhang K-Q, et al. Hot bands of water up to $6\nu_2 - 5\nu_2$ in the 933–2500 cm^{-1} region. J Mol Spectrosc 1999;193:118–36.
[44] Zobov NF, Polyansky OL, Tennyson J, Shirin SV, Nassar R, Hirao T, et al. Using laboratory spectroscopy to identify lines in the K and L-band spectrum of water in a sunspot. Astrophys J 2000;530:994–8.
[45] Tereszchuk K, Bernath PF, Zobov NF, Shirin SV, Polyansky OL, Libeskind NI, et al. Laboratory spectroscopy of hot water near 2-microns and sunspot spectroscopy in the h-band region. Astrophys J 2002;577:496–500.
[46] Coheur P-F, Bernath PF, Carleer M, Colin R, Polyansky OL, Zobov NF, et al. 3200 k laboratory emission spectrum of water. J Chem Phys 2005;122:074307.
[47] Petrova T, Poplavskii Y, Serdukov V, Sinitsa L. Intracavity laser spectroscopy of high-temperature water vapour in the range 9390–9450 cm^{-1}. Mol Phys 2006;104:2692–700.
[48] Zobov NF, Shirin SV, Polyansky OL, Barber RJ, Tennyson J, Coheur P-F, et al. Spectrum of hot water in the 2000–4750 cm^{-1} frequency range. J Mol Spectrosc 2006;237:115–22.
[49] Zobov NF, Shirin SV, Ovsannikov RI, Polyansky OL, Barber RJ, Tennyson J, et al. Spectrum of hot water in the 4750–13000 cm^{-1} frequency range. Mon Not R Astr Soc 2008;387:1093–8.
[50] Yu S, Pearson JC, Drouin BJ, Martin-Drumel M-A, Pirali O, Vervloet M, et al. Measurement and analysis of new terahertz and far-infrared spectra of high temperature water. J Mol Spectrosc 2012;279:16–25.
[51] Polyansky OL, Zobov NF, Viti S, Tennyson J, Bernath PF, Wallace L. Water in the sun: line assignments based on variational calculations. Science 1997;277:346–9.
[52] Mellau GC, Winnewisser M, Maki A. Emission spectrum of HCN at 1400 k in the region of bending fundamental. Fifteenth colloquium on high-resolution molecular spectroscopy, Glasgow; 1997.
[53] Mellau GC, Winnewisser M. High s/n FT-IR emission setup for the range 300–11000 cm^{-1}. Fifteenth colloquium on high-resolution molecular spectroscopy, Glasgow; 1997.
[54] Mellau GC. Fourier-transform-spectroscopy of HCN: measurement and interpretation of new infrared transitions between highly excited states. Doctoral Dissertation in physics at the Justus-Liebig University Gieen; 2003.
[55] Barber RJ, Tennyson J, Harris GJ, Tolchenov RN. A high accuracy computed water line list. Mon Not Royal Astron Soc 2006;368:1087–94.
[56] Jensen P. The potential energy surface for the electronic ground state of the water molecule determined from experimental data using a variational approach. J Mol Spectrosc 1989;133:438–60.
[57] Partridge H, Schwenke DW. The determination of an accurate isotope dependent potential energy surface for water from extensive ab initio calculations and experimental data. J Chem Phys 1997;106:4618–39.
[58] Schwenke DW, Partridge H. Convergence testing of the analytic representation of an ab initio dipole moment function for water: improved fitting yields improved intensities. J Chem Phys 2000;113:6592–7.
[59] Shirin SV, Polyansky OL, Zobov NF, Barletta P, Tennyson J. Spectroscopically determined potential energy surface of $H_2{}^{16}O$ up to 25 000 cm^{-1}. J Chem Phys 2003;308:2124–9.
[60] Barletta P, Shirin SV, Zobov NF, Polyansky OL, Tennyson J, Valeev EF, et al. The CVRQD ab initio ground-state adiabatic potential energy surfaces for the water molecule. J Chem Phys 2006;125:204307.
[61] Shirin SV, Polyansky OL, Zobov NF, Ovsyannikov RI, Császár AG, Tennyson J. Spectroscopically determined potential energy surfaces of the $H_2{}^{16}O$, $H_2{}^{17}O$ and $H_2{}^{18}O$ isotopologues of water. J Mol Spectrosc 2006;236:216–23.
[62] Lodi L, Tolchenov RN, Tennyson J, Lynas-Gray AE, Shirin SV, Zobov NF, et al. A new ab initio ground-state dipole moment surface for the water molecule. J Chem Phys 2008;128:044304.
[63] Grechko M, Boyarkin OV, Rizzo TR, Maksyutenko P, Zobov NF, Shirin SV, et al. State-selective spectroscopy of water up to its first dissociation limit. J Chem Phys 2009;131:221105.
[64] Császár AG, Mátyus E, Szidarovszky T, Lodi L, Zobov NF, Shirin SV, et al. First-principles prediction and partial characterization of the vibrational states of water up to dissociation. J Quant Spectrosc Radiat Transfer 2010;111:1043–64.
[65] Lodi L, Tennyson J, Polyansky OL. A global, high accuracy ab initio dipole moment surface for the electronic ground state of the water molecule. J Chem Phys 2011;135:034113.
[66] Tennyson J, Kostin MA, Barletta P, Harris GJ, Polyansky OL, Ramanlal J, et al. DVR3d: a program suite for the calculation of rotation-vibration spectra of triatomic molecules. Comput Phys Comm 2004;163:85–116.
[67] Miani A, Tennyson J. Can ortho-para transitions for water be observed? J Chem Phys 2004;120:2732–9.
[68] Newman MEJ. Networks. Oxford University Press, Oxford 2010.
[69] Mellau GC, Winnewisser BP, Winnewisser M. Near infrared emission spectrum of HCN. J Mol Spectrosc 2008;249:23–42.